Vibration Compensating Beam Scanning Interferometer for Surface Measurement

X.Jiang[1], H.Martin[1] and K.Wang[1]
[1] University of Huddersfield, Queensgate, Huddersfield HD1 3DH, UK

ABSTRACT

Light beam scanning using a dispersive element and wavelength tuning is coupled with fibre-optic interferometry to realize a new surface measurement instrument. The instrument is capable of measuring nano-scale surface structures and form deviation. It features active vibration compensation and a small optical probe size that may be placed remotely from the main apparatus. Active vibration compensation is provided by the multiplexing of two interferometers with near common paths. Closed loop control of a mirror mounted on a piezoelectric transducer is used to keep the path length stable. Experiments were carried out due deduce the effectiveness of the vibration compensation and the ability to carry out a real measurement in the face of large environmental disturbance.

Keywords fibre interferometer vibration stabilised

1 INTRODUCTION

Technological advances in several fields have resulted in the increased use of nano-scale and ultra-precision surfaces. Such fields include optics, hard disc manufacture, micro molding and micro machining. Multi-axis machining and micro-fabrication techniques are seeing surfaces with sub-micron form accuracy and the production of nano-scale surface features. With ever decreasing manufacturing scales the current state of online metrology methods is found to be lacking. Light scattering methods are numerous and well established, they can give a qualitative idea of overall surface roughness and are in generally suitable for in-situ measurement. Unfortunately they cannot provide traceability as they work using fitting and statistical interpretation. Additionally, they are all area averaging techniques and so cannot be used to discern micro-structures [1-4]. Other novel methods are either limited in scope or resolution [5,6].

Optical interferometric techniques for metrology hold many advantages such a speed, resolution, traceability and non-contact measurement. They are not however very suitable for the application to on-line measurement due to the fact that any height disturbance is mapped directly onto the measurement result. This research hopes to try and alleviate this issue by providing immunity to disturbance during the measurement interval by way of active vibration compensation, thus realizing an instrument with the benefits of an optical interferometer, but which is suitable for on-line applications.

One of the central requirements for the development of the multiplexed fibre interferometer is the ability to place it on-line, in a workshop environment. Clearly such a requirement presents difficulties for precision measurement where usually the environment is a vibration isolated, temperature stabilized clean room. The challenge to try and create a device to measure accurately and repeatably under workshop conditions is a major one.

2 PRINCIPLE

The key feature of the multiplexed fibre interferometer is the combination of two interferometers operating at different wavelengths but which follow a common path for the majority of their length. The paths separate only at the optical probe, at which point they are laterally displaced along a profile on the measurand surface. Any vertical movement of the measurand due to vibration will change the optical path length of both interferometers equally. Additionally, any path length change elsewhere in the interferometer due to temperature variation will also affect both interferometers equally.

Using one of the interferometers as a reference interferometer at a fixed wavelength, we can measure the fluctuations in optical path length due to these external factors. Furthermore, the use of an actuator to alter the path length in one of the arms will induce an identical path length change in both interferometers. Closed loop control can be applied using the fixed wavelength reference interferometer output as the feedback source. When employed, the closed loop control can lock the reference interferometer path length at any point and hold it there in the face of disturbance. By virtue

of the near common path configuration, this will in effect hold the second, measurement interferometer steady as well. This measurement interferometer is now free to perform the required measurement in a stable fashion [7].

The reference interferometer also provides the ability to implement accurate phase shifting interferometry techniques in order to retrieve the phase data from the measurement interferometer output. The mirror may be moved very accurately using the same closed loop feedback method as for vibration cancellation.

The actual surface measurement is performed by sweeping the light beam of the measurement interferometer along a profile on the surface. This is facilitated by tuning the source wavelength, and placing a blazed diffraction grating in the beam path. The first order beam is thus used as an optical stylus. The interference signal is sampled and digitized during the sweep to provide a discrete set of intensity values for each sampled point on the swept profile.

Extraction of phase data from the output of an interferometer is non-trivial due the co-sinusoidal nature of the response. Phase shifting interferometry (PSI) is used to discern the actual phase value [8].

In our method the measurement interferometer source wavelength is tuned to provide the beam scanning, and the resulting intensity values produced by the scanned profile are sampled. After each beam sweep, a phase shift is induced by moving the piezo-electric translator (PZT) mounted reference mirror. We thus retrieve four sets of intensity data, each containing the intensity values for the same scanned profile but at different phase shifts. If $\varphi(x)$ is the original phase at a sampled point x on the scan profile, the phase is altered by 4 equal steps; -3α, -α, α and 3α around this point and 4 intensity values are obtained, $I_1(x)$, $I_2(x)$, $I_3(x)$ and $I_4(x)$ respectively. These can then be input into the Carré PSI algorithm to yield the original phase value at each profile point, x;

$$\varphi(x) = \tan^{-1}\sqrt{\frac{\left(3I_2(x)-3I_3(x)-I_1(x)+I_4(x)\right)\left(I_1(x)+I_2(x)-I_3(x)-I_4(x)\right)}{\left(I_1(x)-I_2(x)-I_3(x)+I_4(x)\right)^2}} \qquad (1)$$

The most effective phase shifting angle to provide the greatest immunity from random, non-systematic intensity noise (thus reducing lost data points) has been shown to be 110° thus α is set to 55° [9].

With closed loop control it is possible to lock the reference interferometer at any point on the reference fringe simply by adjusting the set-point voltage applied to the PI controller. This method greatly reduces error due to the large non-linearities present in all PZTs.

3 APPARATUS

Figure 1 shows the experimental setup of the interferometer. A laser diode and the tunable laser source (TLS) illuminate the reference and measurement interferometers respectively. The laser diode operates at a wavelength of 1550nm and the TLS is operated between 1560 nm and 1580 nm. Both sources are multiplexed into the same fibre by a 3dB coupler. A combination of a reflective diffraction grating and collimating objective lens provides the ability to scan the measurement beam across the surface of the measurand, by tuning the source wavelength. De-multiplexing of the two interferometer sources is performed by a combination of a circulator and fibre bragg grating (FBG). After de-multiplexing, the intensity of each interference signal is interrogated by a fibre pigtailed PIN detector.

The actual interferometer is a Michelson configuration using a blazed diffraction grating (Jobin Yvon 510 97 020) with the reflected zero order beam and the diffracted first order beam providing the two beam paths. Light from the input fibre is collimated onto the diffraction grating using a graded index (GRIN) lens, which serves also to couple the returning light beam back into the fibre. On retro-reflection from the reference mirror and the measurand surface, they recombine on the grating. A blazed grating is used to shift more of the source light power to the measurand (first order) surface beams as it is reasonable to expect that this surface would generally be less reflective than the reference mirror. An achromatic doublet (Melles Griot LAI007) is used to collimate the diffracted beam onto the measurand surface. When the wavelength of the diffracted beam is tuned the measurement beam sweeps laterally across the surface. Clearly, the lateral resolution of the instrument is a limited by the focused measurement beam diameter. The wavelength change, $\Delta\lambda$ of the tunable laser (Ando Electric Co. AD4320D) is from 1560 nm to 1580 nm which with the current optics yields a scan length of approximately 3mm.

A data acquisition (DAQ) card (National Instruments NI PCI-6221) samples the measurement interferometer output during the wavelength sweep generating a data array with each element representing the interferometer intensity at each point on the scanned profile. The reference

interferometer measurement beam remains in the same spot on the surface during the profile scan since its wavelength remains constant at 1550nm. The output of each interferometer is analysed using two separate PIN detectors. The PIN detectors are operated with no reverse voltage bias in order to reduce excess shot noise resulting from dark current flow. This is reasonable as high speed operation is not a priority in this application. Each PIN detector is interrogated by transimpedance amplifier which provides high gain current to voltage conversion.

A low voltage piezoelectric translator (PZT) stack is utilised (PI 820.10) to move the reference mirror which provides a displacement of 15µm/100V. This means with a ±15V control voltage range we can apply approximately 4.5µm of displacement thus providing 6 full fringes of compensation range.

State of polarisation (SOP) evolution in single mode optical fibres can be a major source of error in any interferometric optical fibre sensor. The subject has been well studied and many methods for overcoming such effects have been suggested [10]. The arms of a fibre interferometer can be modelled as a lumped birefringence R_{r-m} of rotational magnitude (phase delay) Ω_{r-m}. The visibility of the interferometer output is a function of the angle, θ subtended by the great circle joining the input SOP and the lumped birefringence $R_{r-m}(\Omega_{r-m})$, as represented on the Poincaré sphere [11]. In the case for our instrument, the arms are free space optics thus $R_{r-m}(\Omega_{r-m})$ remains approximately static. As such it is only the variation of the input SOP that alters the value of θ. The dependence of visibility on θ is seen to be,

$$V = \left\{1 - \sin^2\theta \cdot \sin^2\left(\Omega_{r-m}/2\right)\right\}^{1/2} \tag{2}$$

It has also been shown that phase error in the output of an interferometer may also be produced by SOP variation and that this phase error is most pronounced when the visibility is at a minimum. Thus the best operating conditions for a fibre interferometer in terms of both signal to noise ratio and polarisation induced phase noise is to ensure that the visibility is maximised.

Pseudo un-polarised light as produced by a polarisation scrambler, assuming the frequencies of interest are much lower than the scrambling frequency, can be used to reduce visibility variance due to SOP evolution in the input fibre. We used an all-fibre polarisation scrambler (Fibre Pro PS-155A) which has a scrambling rate of 200 kHz. This resulted in a much improved stability from input lead perturbation at the cost of slightly reduced visibility. In addition, all fibres were taped down to the optical table in order to reduce movement wherever possible. Currently, the position of a fibre loop on the optical table is adjusted to obtain an approximate maximum visibility value before the scrambler is switched on [12].

A digital control method using the flexibility of a dedicated digital signal processing (DSP) device means that the process of changing parameters, altering controller structures and adding filters can be done by simply altering software. Stability of parameters due to environmental change is also greatly improved. It also opens up the possibility of using adaptive algorithms in the future to enhance performance. A standard PID algorithm is shown below in recurrence form;

$$y_n = y_{n-1} + K_p\left[\left(1 + \frac{T_s}{T_i} + \frac{T_d}{T_s}\right)e_n - \left(1 + 2\frac{T_d}{T_s}\right)e_{n-1} + \frac{T_d}{T_s}e_{n-2}\right] \tag{3}$$

Where y is the control signal sent to the PZT and e the error signal derived from the difference between the setpoint and the actual output of the interferometer. T_i and T_d are the integration time and differential gain respectively and K_P is the controller overall gain. The sampling interval is T_s which must be much higher than the frequencies of interest.

The algorithm (3) was implemented using a Texas Instruments TMS320F2812 digital signal controller and code was produced using a dedicated C-compiler. It is a 32 bit fixed point processor and runs at up to 150 million instructions per second (MIPS). An interface board was also constructed to provide the analogue control signal using a 16bit digital to analogue converter (Analog Devices AD766JN). The board also provided a transimpedance amplifier and digital input/output also. The tuning of the discrete PID controller was done with the derivative action turned off, essentially providing a PI controller.

4 RESULTS AND DISCUSSION

In order to determine the effectiveness of the vibration compensation two experiments were carried out. First, a sinusoidal disturbance of 300nm peak to peak was applied to the measurement mirror using a PZT. The disturbance was centred about the quadrature point and its magnitude recorded. The active vibration compensation was then switched on and the interferometer locked to the quadrature point, a reduced magnitude being observed. The experiment was repeated at gradually increasing frequencies. Figure 2 shows the attenuation of the disturbance observed at the output of the measurement interferometer when the vibration compensation was switched on relative to the uncompensated signal. The reduced effectiveness of the vibration compensation at the higher frequencies is due to the limited slew rate of the PZT. This could be improved by using a stiffer, pre-loaded PZT and applying the full scale voltage range with a suitable PZT driver.
A second experiment was carried out to determine the ability of the system to take measurements in the face of induced disturbance. A step height sample measured with the system. A large scale 50Hz sinusoidal disturbance of 750nm peak to peak was applied to the measurand. Such a disturbance accounts for approximately a full fringe of disturbance around the operating wavelength and as such would completely obscure any height data obtained in any uncompensated interferometer. The step height was first measured by the interferometer with no disturbance applied and the resultant phase profile is shown in figure 3(a). It was then measured again with the disturbance applied to the measurand; the results are shown in figure 3(b). Due to the fact that the phase stepping and the active vibration compensation are both controlled by the same closed loop feedback, it is impossible to make a measurement without also having the vibration compensation active. We cannot therefore show the worst case result of the disturbed step height sample with no vibration compensation present.
With the view that most building disturbance frequencies tend to be below a few 100 Hz, the system shows great promise. However, by increasing the frequency response of the compensation system we will be able to better improve the response and high frequencies and further reduce the error at the low end. Preliminary experiments have been performed with and electro-optic modulator (EOM) with this aim in mind.

5 IMPROVING PERFORMANCE AND FUTURE WORK

An electro-optic modulator (EOM) is capable of providing very rapid variation in its refractive index when a strong electric field is applied across it. By placing an EOM in the arm of an interferometer it can be used to vary alter the phase in that arm as the refractive index change in the crystal alters the optical path length. It can be seen that this effect has the same effect as a mirror mounted on a PZT but there is no physical movement involved and access times are much quicker.
An electro-optic modulator (EOM) is capable of providing very rapid variation in its refractive index when a strong electric field is applied across it. By placing an EOM in the arm of an interferometer it can be used to vary alter the phase in that arm as the refractive index change in the crystal alters the optical path length. It can be seen that this effect has the same effect as a mirror mounted on a PZT. However, there are no moving parts involved and access times are much quicker. A few such interferometric systems have been developed already but the main limitations are the expense and difficulty of driving them [14]. Phase retardation capabilities are characterised by the half-wave voltage, V_π of the EOM. Typical values of V_π for bulk optic EOMs are in the range of 300V at operating wavelengths of 1600nm and they represent highly capacitive loads [42]. The large slew rates and current supply requirements thus make very high speed operation very difficult.
Communications technology provides a cheaper and much improved solution that may be integrated into a fibre optic interferometer to provide the same stabilisation feature. Integrated optic phase modulators perform the same function as there bulk counterparts, but due to the long length of the waveguide compared to its narrow width, values of V_π can be as low as 3V. They present a small capacitive load (typically a few pF), which means that the driving electronics can be very simple and modulation speeds of up to several GHz can be obtained.
The EOM used features a V_π of <5V (at 1550nm operating wavelength) and is capable of being driven across a range of ±30V. This yields a phase range of approximately 12π radians, the equivalent of path change of 4.65 μm.
An integrated optic EOM supplies two major advantages over a PZT/mirror based methods. Very fast frequency response means that higher frequency disturbance may be compensated for and open up the possibility of implementing phase shift techniques at very fast rates and allowing pseudo real-time phase readouts from the system.

The scheme remains, in its physical setup, very similar to the previous one and is shown in figure 5. The key difference is that the reference mirror is now fixed and an EOM is placed in the reference fibre path. Phase shifting is now performed applying a stepped input voltage to the EOM, each step relating to the required phase shift. The stepping rate is limited by the rise/fall times of the EOM and its driver (typically <10μs) as well as the frequency response of the PIN detector used.
PSI techniques at such high rates will result in enhanced accuracy as the disturbance between shifts will be less. In addition, no mechanical parts mean vibration due to mirror movement is eliminated, as are errors due to PZT non-linearity. It is feasible to operate the phase stepping system in an open loop configuration, as long as the proper calibration is performed prior to the measurement.
With such high retrieval rates for real phase data, the possibility of stabilisation using this technique now becomes apparent. As the DSP can sample and process the outputs of the measurement and reference interferometers simultaneously. The real phase data from the reference interferometer can be used to keep the OPD of the interferometers arms stable by adjusting the DC bias of the stepped waveform applied to the EOM. Stabilisation can be carried out with a PID algorithm, using the DSP, with calculated phase data from the reference interferometer providing the error signal source. Measurement data can be stored on board the DSP and read out over an RS232 interface or similar at the end of the measurement cycle. Clearly it is the DSP that will be the bottleneck in this system, but very fast 3-step phase shifting algorithms designed specifically for realtime embedded applications have been developed [15]. Figure 5 illustrates the rapid phase shifting technique.
The results from preliminary tests with a custom built EOM (Eospace inc.) are promising. A setup similar to that shown in figure 4 was setup, but without the tuneable laser or FBG de-multiplexer. This provided an all-fibre Michelson interferometer running at a fixed wavelength of 1550nm. Initial observations were that path length change in the all fibre configuration of the arms due to disturbance and temperature drift was greatly increased as expected [16]. A square wave was used to drive the EOM over approximately one full fringe of movement and the results were recorded by a digitizing oscilloscope, see figure 7(a). The open loop response of the PZT was also recorded for comparison and the results are shown in figure 7(b). The rise time for the EOM is approximately 25μs as opposed about 1ms for the PZT. A further experiment to directly modulate the laser diode intensity showed that the response was limited by the photodiode/transimpedance amplifier configuration, not the EOM. We thus expect to see even greater increases in response speeds once the receiver has been optimised.
While response speeds are much improved with this method, stability issues due to SOP evolution will be much pronounced. The all-fibre configuration in the individual arms means that visibility fading due to varying birefringence in the arms is apparent. This cannot be improved upon by the use of a polarisation scrambler, unlike in the previous setup. Another problem is that an inline linear polarizer is used in the EOM to ensure that only the phase shifted polarisation makes it through the interferometer arm. The result of this is that SOP evolution in the input lead now leads directly to an output intensity shift (as opposed to a visibility shift). Further research work will clarify the situation and the introduction of polarisation maintaining fibres could go a long way to alleviating this problem.

REFERENCES

[1] Vorburger, T. and Teague, E., "Optical techniques for on-line measurement of surface topography", Precision Engineering 3(2), 61-83 (1981).
[2] Vorburger, T., Marx, E. and Lettieri, T., "Regimes of surface roughness measurable with light scattering", Appl. Opt. 32, 3408 (1993).
[3] Creath, K., "Phase-shifting speckle interferometry", 24, 3058 (1985).
[4] Tay, C., Wang, S., Quan, C. and Shang, H., "In situ surface roughness measurement using a laser scattering method", Optics Communications 218 (2003), 1-10.
[5] Kuwamura, S., Yamaguchi, I., "Wavelength scanning profilometry for real-time surface shape measurement", Appl. Opt. 36, 4482 (1997).
[6] Yamamoto, A. and Yamaguchi, I., "Profilometry of SIoped Plane Surfaces by Wavelength Scanning Interferometry", Optical Review 9(3), 112-121 (2002).
[7] X. Jiang, K. Wang, and H. Martin, "Near common-path optical fibre interferometer for potentially fast on-line microscale-nanoscale surface measurement," Opt. Lett. **31**, 3603-3605 (2006).
[8] K. Creath, "Phase-Measurement Interferometry Techniques," in *Progress in Optics*. XXVI, E. Wolf, ed. (Elsevier Science Publishers, Amsterdam,1988), pp.349-393.
[9] Kemao, Q., Fangjun, S., and Xiaoping, W., "Determination of the best phase step of the Carré algorithm in phase shifting interferometry", Meas. Sci. Technol. 11, 1220–1223 (2000).
[10] Heidrich, H., Hoffman, D. and Noé, R., "Endless Polarisation Control Systems for Coherent Optics", J. Lightwave Technology 6(7), 1199-1208 (1988).

[11] Johnson, M., "Poincaré representation of birefringent networks", Appl. Opt. 20(12), 2075-2080 (1981).
[12] Kersey, A., Marrone, M. and Dandridge, A., "Analysis of Input-Polarisation-Induced Phase Noise in Interferometric Fibre-optic Sensors and Its Reduction using Polarisation Scrambling", J. Lightwave Technology 8(6), 838-845 (1990).
[13] Hang, C.C., Tan, K.K., and Wang, Q., "*Advances in PID control*", London : Springer, pp. 99-187 (1999).
[14] Zhou, C. and Burge, J., "Vibration compensated interferometer for surface metrology", App. Opt. 40, 6215.
[15] Huang, P.S. and Zhang, S., "Fast three-step phase-shifting Algorithm", Appl. Opt. 45(21), 5086-5091 (2006).
[16] Jackson, D.A., Priest, R., Dandridge, A., and Tveten, A.B., "Elimination of drift in a single-mode optical fibre interferometer using a piezoelectrically stretched coiled fibre", Appl. Opt. 19(17), 2926-2929 (1980).

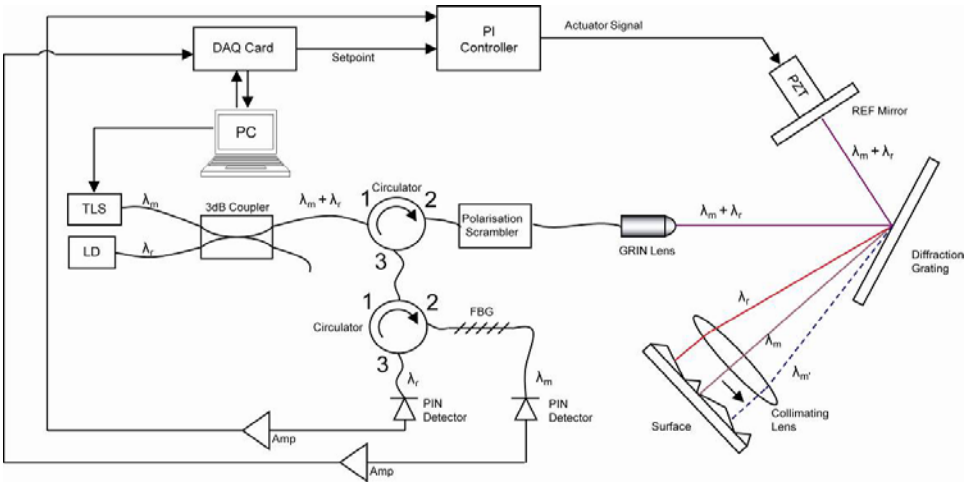

Figure 1 Experimental Setup

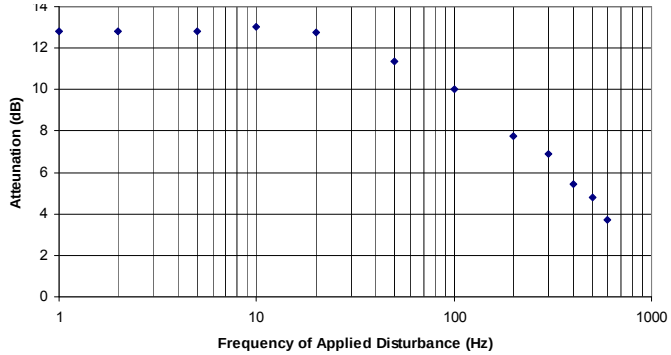

Figure 2 Effectiveness of Vibration Compensation

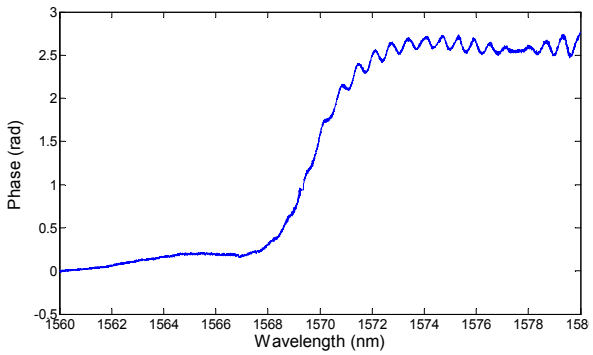

Figure 3(a) Step height

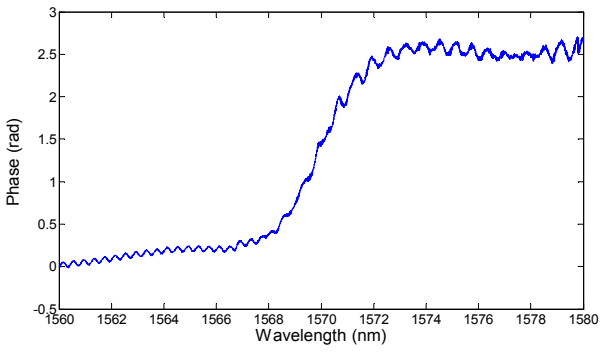

Figure 3(b) Step Height Response with added Disturbance

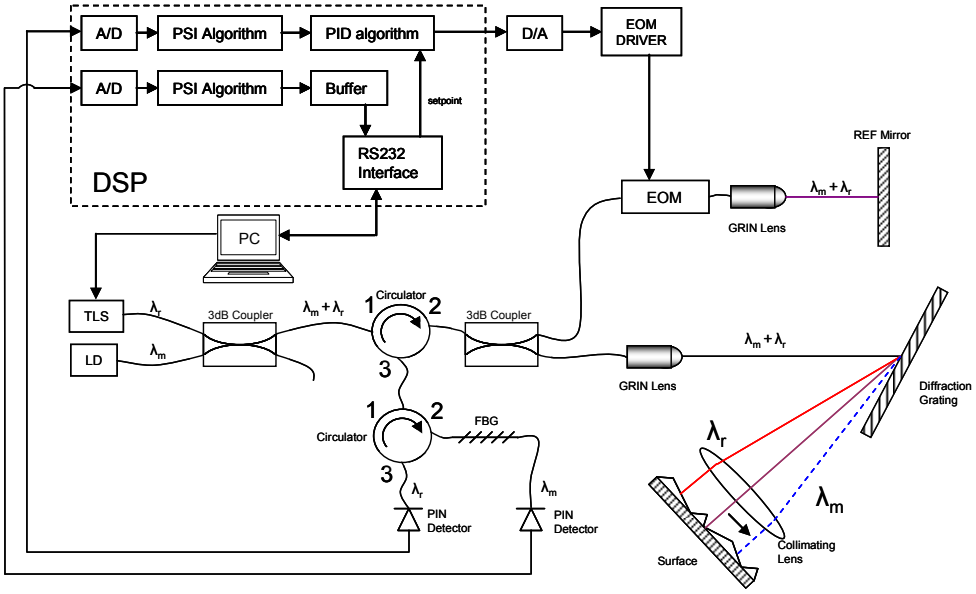

Figure 4 EOM Setup

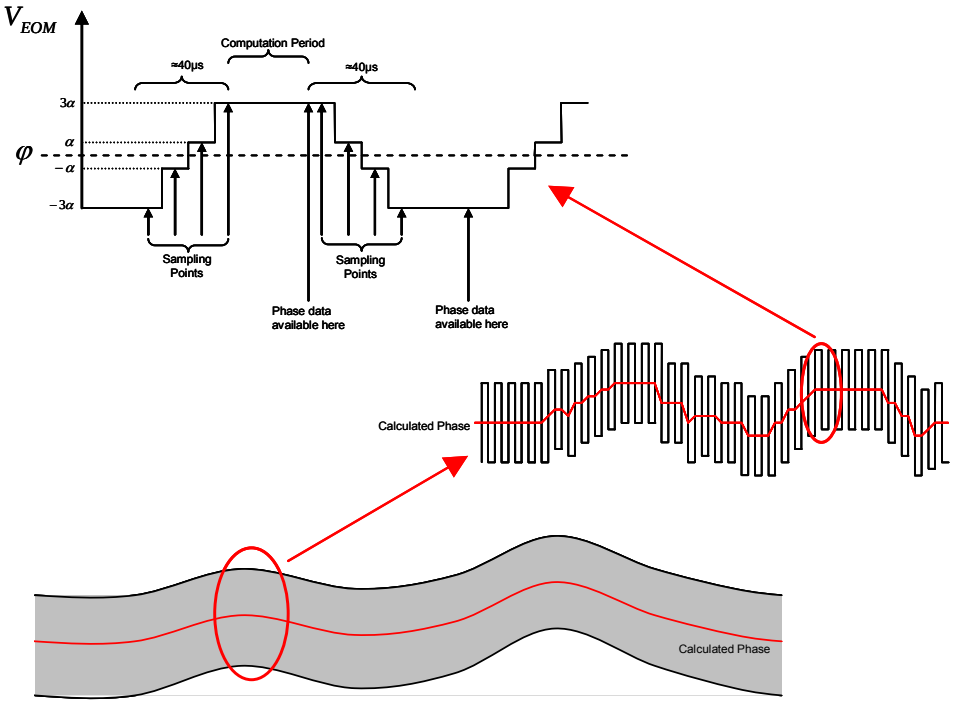

Figure 5 Rapid Phase Shifting Technique

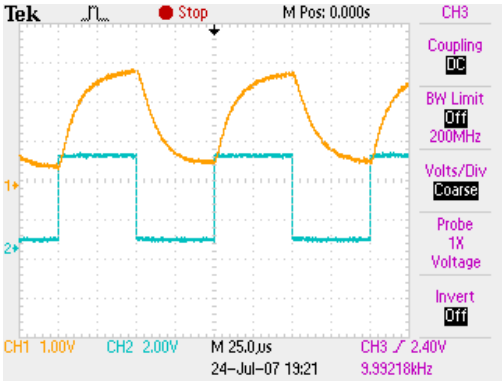

Figure 7(a) EOM Step Response

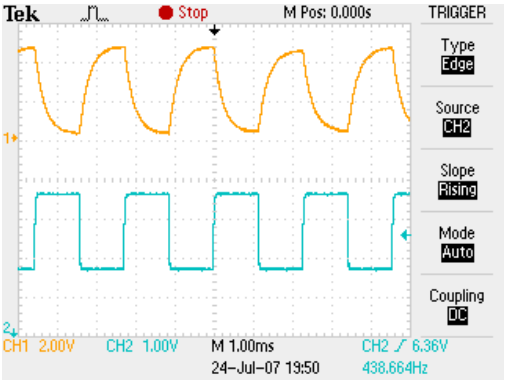

Figure 7(b) PZT Step Response